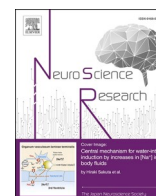







Contents lists available at ScienceDirect

Neuroscience Research

journal homepage: www.sciencedirect.com/journal/neuroscience-research

Time-window of offline long-term potentiation in anterior cingulate cortex during memory consolidation and recall

Junyu Liu^{a,1} , Akihiro Goto^{a,b,c,2} , Yasunori Hayashi^{a,*,3} ^a Department of Pharmacology, Kyoto University Graduate School of Medicine, Kyoto 606-8501, Japan^b Hakubi Center for Advanced Research, Kyoto University, Kyoto 606-8501, Japan^c PRESTO, Japan Science and Technology Agency (JST), Tokyo, Japan

ARTICLE INFO

Keywords:

memory consolidation
synaptic plasticity
long-term potentiation
anterior cingulate cortex
cofilin

ABSTRACT

Episodic memories are initially formed in the hippocampus and subsequently transferred to cortical regions for long-term storage. This process, known as memory consolidation, involves plastic changes in synaptic transmission such as long-term potentiation (LTP). However, at what time points and specific locations LTP acts at remains unclear. We previously developed an optogenetic tool, cofilin-SuperNova (CFL-SN), that allows for the selective erasure of LTP within a limited time window. Using CFL-SN, here we show that the erasure of LTP in the anterior cingulate cortex (ACC) during sleep on the subsequent day, but not immediately following task acquisition, impairs recall of memory. However, allowing a single day without perturbation allowed memory to be recalled. Even after 7 days of repeated erasure of LTP, allowing LTP in the ACC on the 8th day restores memory recall. Once the memory is transferred, further LTP in the ACC is not necessary. Our findings indicate that the memory consolidation process completes in one sleep cycle and can occur at any timepoint up to 8th day.

1. Introduction

Episodic memories are initially formed in the hippocampus but are subsequently transferred to cortical areas for long term storage, in a process termed memory consolidation (Frankland and Bontempi, 2005; Goto, 2022; Sakaguchi and Hayashi, 2012; Tonegawa et al., 2018). Among the multiple brain regions, the anterior cingulate cortex (ACC) has been implicated as a target area critical for the long-term preservation of memories. This is supported by observations that the ACC is reactivated upon the recall of remote memories as revealed by staining of the immediately early gene product c-Fos, and that activation of ACC is required for execution of memory-related behavior (Bero et al., 2014; Bontempi et al., 1999; Frankland et al., 2004; Goto et al., 2021; Jhang et al., 2018). In agreement with these data, the ACC is ideally situated to serve as an integrative center of remote memory, since it receives multiple modalities of sensory information, including visual, auditory, and

somatic and projects to various brain regions, including the amygdala, periaqueductal grey, and nucleus accumbens, capable of triggering behavioral responses (Rolls, 2023; Smith et al., 2021; Wu et al., 2023).

Experimental evidence suggests memory consolidation is initiated immediately following an event and concludes within a few weeks (Kitamura et al., 2017; Toader et al., 2023), with long-term potentiation (LTP) of synaptic transmission playing a key role in this process. Heterozygous knockout mice of Ca^{2+} /calmodulin-dependent protein kinase II α subunit (CaMKII α), a serine/threonine protein kinase critical for LTP, exhibit abnormal cortical LTP, though hippocampal LTP remains intact (Frankland et al., 2001). Consistent with this, these animals exhibit normal memory 3 days after learning, but show impairments when tested 10–50 days later. Separately, a recent study used the ratio of α -amino-3-hydroxy-5-methyl-4-isoxazolepropionic acid (AMPA) to *N*-methyl-D-aspartate (NMDA) type glutamate receptor mediated synaptic currents (AMPA/NMDA ratio) as an index, to demonstrate that

Abbreviations: ACC, anterior cingulate cortex; CALI, chromophore-assisted light inactivation; LTP, long-term potentiation; CaMKII, Ca^{2+} /calmodulin-dependent protein kinase; AMPA, α -amino-3-hydroxy-5-methyl-4-isoxazolepropionic acid; NMDA, *N*-methyl-D-aspartate; CFL, cofilin; SN, supernova; DIO, double-foxed cassette; IA test, inhibitory avoidance test.

* Corresponding author.

E-mail address: yhayashi-tyk@umin.ac.jp (Y. Hayashi).

¹ 0000-0002-3803-4068

² 0000-0002-1753-2893

³ 0000-0002-7560-3004

<https://doi.org/10.1016/j.neures.2024.12.009>

Received 17 November 2024; Received in revised form 22 December 2024; Accepted 24 December 2024

Available online 27 December 2024

0168-0102/© 2025 The Authors. Published by Elsevier B.V. This is an open access article under the CC BY license (<http://creativecommons.org/licenses/by/4.0/>).

Please cite this article as: Junyu Liu et al., *Neuroscience Research*, <https://doi.org/10.1016/j.neures.2024.12.009>

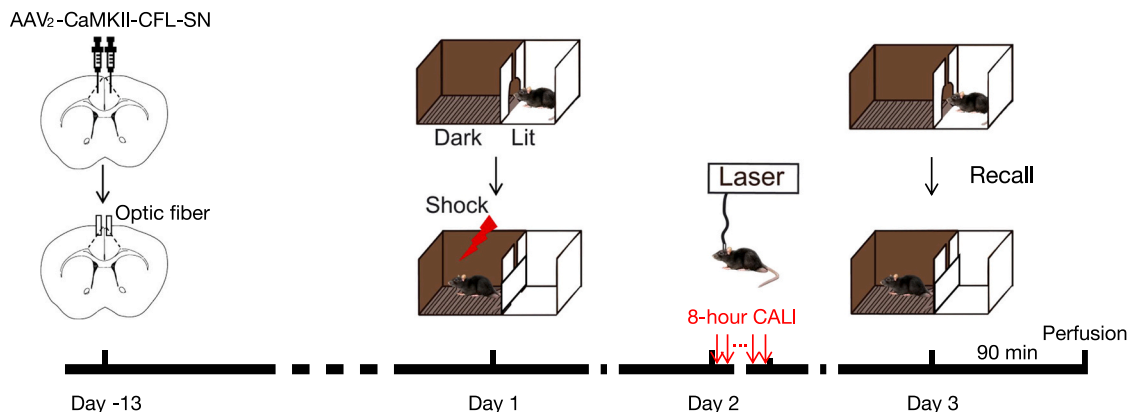


Fig. 1. An example of experimental scheme. AAV₂-CaMKII-CFL-SN was injected into the ACC of a WT mouse and a dual-fiber cannula was implanted over ACC 14 days prior to the behavior test. The mice were exposed to the lit side of the chamber and then allowed to explore the dark side of the chamber, where they received a footshock 10 seconds after they stepped in. On day 2, the mice were illuminated with a 593 nm laser for 30 seconds every 20 minutes during 8 hour period in home cage. Memory was tested on day 3 by reintroducing them in the same context without footshock and measuring the crossover latency to the dark side. Perfusion was conducted 90 minutes after the recall.

synapses in the ACC remained potentiated 28 days after learning (Lee et al., 2023). However, it is still largely unclear when and where LTP takes place and what triggers the memory consolidation process.

Based on our original findings that cofilin, an filamentous (F-)actin binding protein, is rapidly translocated to the synapse upon LTP induction and maintains the enlarged dendritic spine (structural LTP or sLTP), we demonstrated that optical disruption of cofilin can erase sLTP, as well as electrically recorded LTP of AMPAR transmission (Bosch et al., 2014; Goto et al., 2021). This was accomplished by fusing cofilin with SuperNova (CFL-SN), a photosensitizer protein which allows chromophore-assisted light inactivation (CALI) of a protein it is fused with, upon light illumination (Goto et al., 2021; Kim et al., 2015; Takemoto et al., 2013). The effects of CALI of CFL-SN are limited to a 30-minute window following the induction of structural LTP. If CALI is conducted before LTP is induced, or 50 minutes later, sLTP remains intact. Importantly, CALI of CFL-SN does not impact unstimulated synapses. In-vivo testing of CFL-SN as an optogenetic tool, showed that LTP can be retroactively erased within a 20-minute time window, allowing us to determine the timing and location where LTP occurs post-learning. Using this tool, we demonstrated that LTP takes place both online and offline (Goto et al., 2021). The first wave of LTP, online LTP, takes place in hippocampus during learning, followed by another wave of LTP, offline LTP, in the subsequent sleep. Notably, LTP did not occur in the ACC during these periods but did emerge during sleep on the following day (Goto et al., 2021). However, it remains unclear how long information remains accessible after learning, if the episode-specific LTP in ACC is blocked. To address this, we aimed to identify the specific time window of LTP in the ACC that is crucial for memory consolidation.

2. Materials and methods

2.1. Mice

Animal experiments were conducted in accordance with the guidelines set by the Committee for Animal Care of Kyoto University. Wild-type C57BL/6 JmsSlc (SLC) and CaMKII α -Cre transgenic mice (Jackson Laboratory; Camk2a-cre) T29-1St1, back crossed with C57BL/6J (Tsien et al., 1996) were used in this study. All mice were male, aged between 10 and 16-week-old and were housed on a reverse 12-hour light/dark cycle (lights on at 21:00 and off at 9:00), in groups of two to five per cage with littermates. They were allowed *ad libitum* access to food and water. Post surgery, mice were housed separately in individual cages to avoid damage to the implant by cagemates.

2.2. Preparation of adeno-associated viral vectors

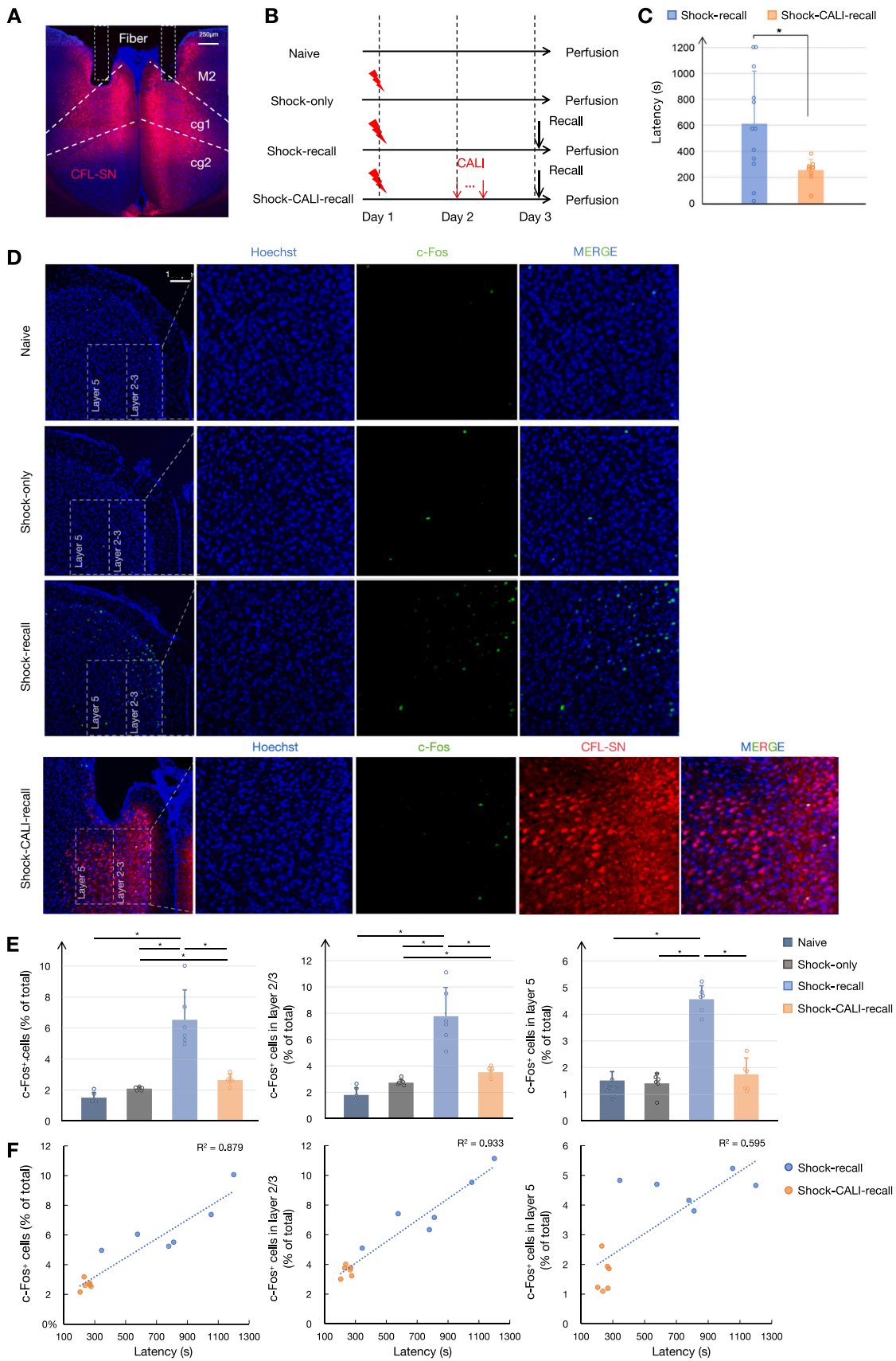
pAAV-CaMKII-CFL-SN was constructed by replacing the EF1 α promoter and double-floxed cassette (DIO) in the pAAV-EF1 α -DIO-CFL-SN plasmid (Addgene #181740) with the CaMKII α promoter. Both the AAV₂-EF1 α -DIO-CFL-SN and AAV₂-CaMKII-CFL-SN were purified using iodixanol gradient ultracentrifugation (Grieger et al., 2006). Viral titers were 1.3×10^{13} and 7.2×10^{12} genome copies per ml respectively and were aliquoted and stored at -80°C until use.

2.3. Stereotactic injection and optic fiber implantation

Mice were anesthetized with isoflurane and their heads fixed in a stereotactic apparatus. Virus solution was bilaterally injected using a capillary glass micropipette connected to a microsyringe (MS-10; Ito) via a tube filled with liquid paraffin, at a rate of 60 nL/min. 200–250 nL of the solution was injected into the ACC at following coordinates: + 0.8 mm AP, 0.2 mm ML, and 1.4 mm DV, relative to bregma. Once complete, the micropipette remained in place for an additional 15 minutes before being withdrawn. Dual fiber-optic cannulas (DFC_200/240-0.22_3mm_GS0.7_FLT; Doric Lenses) were then implanted 0.2 mm above the injection site. Lastly, three anchor screws were fixed into the skull and a layer of adhesive cement (Shofu Dental) was applied around the cannulas. Ketoprofen was administered at 1 mg/kg as a post-surgery analgesic.

2.4. Inhibitory avoidance test and CALI

The inhibitory avoidance (IA) apparatus was composed of a lit chamber (length, 17 cm; width, 10 cm; height, 21 cm; white wall) adjoined to a dark chamber (length, 20 cm; width, 10 cm; height, 21 cm; black wall), linked by a sliding door. The lit chamber had a white cardboard floor and was illuminated with white light (25 klx), while the dark chamber had a metal grid floor and was illuminated with 940 nm infrared light. Prior to all experiments, the chambers were cleaned using 70 % ethanol. Mice were placed in the lit chamber for 1 minute, after which the sliding door was opened. Once the mouse stepped with four paws into the dark chamber, the door was closed and an electric footshock was delivered 10 seconds later (CaMKII-Cre mice: 0.90 mA, 50 Hz, 3 seconds, duration of pulse at 1 millisecond; wild-type mice: 1.05 mA, 50 Hz, 4 seconds, duration of pulse at 1 millisecond). Mice were confined to the dark chamber for an additional 1 minute post-shock, before being returned to their home cage. In the memory recall phase, the protocol was repeated but without administering the electric



(caption on next page)

Fig. 2. Optical erasure of memory by CALI on day 2. Distribution of CFL-SN expression in the ACC neurons in a wild type mouse injected with AAV₂-CaMKII-CFL-SN. Dashed rectangles indicate the tracts caused by optical fibers. M2, supplementary motor cortex; cg1, cingulate cortex area 1; cg2, cingulate cortex area 2. **(B)** Experimental protocols: naïve, shock-only (mice without injection or surgery, but with shock), shock-recall (mice without injection or surgery, but with shock and recall), and shock-CALI-recall (mice expressing CFL-SN, shocked, illuminated and with recall). **(C)** Impaired memory by CALI. The Wilcoxon rank-sum test showed a significantly decreased crossover latency in shock-CALI-recall group comparing to shock-recall group ($n_{\text{shock-recall}} = 12$; $n_{\text{shock-CALI-recall}} = 8$; $p = 0.009$; $\alpha = 0.05$). **(D)** c-Fos immunostaining in ACC neurons in the naïve, shock-only, shock-recall, and shock-CALI-recall groups. **(E)** Summary c-Fos immunostaining (left) in all layers using the Wilcoxon rank-sum test ($n_{\text{naïve}} = 6$ mice; $n_{\text{shock-only}} = 6$ mice; $n_{\text{shock-recall}} = 6$ mice; $n_{\text{shock-CALI-recall}} = 6$ mice. $p_{\text{naïve v.s. shock-only}} = 0.009$; $p_{\text{naïve v.s. shock-recall}} = 0.002$; $p_{\text{naïve v.s. shock-CALI-recall}} = 0.002$; $p_{\text{shock-only v.s. shock-recall}} = 0.002$; $p_{\text{shock-only v.s. shock-CALI-recall}} = 0.004$; $p_{\text{shock-recall v.s. shock-CALI-recall}} = 0.002$), as well as those separating by layer 2/3 (middle; $p_{\text{naïve v.s. shock-only}} = 0.009$; $p_{\text{naïve v.s. shock-recall}} = 0.002$; $p_{\text{naïve v.s. shock-CALI-recall}} = 0.002$; $p_{\text{shock-only v.s. shock-recall}} = 0.002$; $p_{\text{shock-only v.s. shock-CALI-recall}} = 0.004$; $p_{\text{shock-recall v.s. shock-CALI-recall}} = 0.002$) and layer 5 cells (right; $p_{\text{naïve v.s. shock-only}} = 0.132$; $p_{\text{naïve v.s. shock-recall}} = 0.002$; $p_{\text{naïve v.s. shock-CALI-recall}} = 0.589$; $p_{\text{shock-only v.s. shock-recall}} = 0.002$; $p_{\text{shock-only v.s. shock-CALI-recall}} = 0.699$; $p_{\text{shock-recall v.s. shock-CALI-recall}} = 0.002$). The α threshold was set at 0.0083 (0.05/6). A higher proportion of c-Fos⁺ cells was observed in layer 2/3 compared to layer 5 ($p_{\text{naïve}} = 0.009$; $p_{\text{shock-only}} = 0.002$; $p_{\text{shock-recall}} = 0.004$; $p_{\text{shock-CALI-recall}} = 0.002$), and α threshold was set at 0.05. **(F)** The crossover latency of recall on day 3 significantly correlated with the proportion of c-Fos⁺ cells in the ACC (left; $p < 0.001$; $R^2 = 0.879$), as well as layer 2/3 (middle; $p < 0.001$; $R^2 = 0.933$) and layer 5 (right; $p = 0.004$; $R^2 = 0.595$).

footshock. The crossover latency of each mouse was measured from the time the door was opened until the animal placed all four paws in the dark chamber.

IA training was conducted at 21:30, the beginning of diurnal period when the sleep cycle starts. On subsequent day(s) each mouse was lightly anesthetized with isoflurane prior to CALI and optical fibers were connected through the cannulas in their head. This allowed light to be delivered through optical fibers and a custom rotatory joint while the mice remained in their home cages. CALI was started at 22:00 using 593 nm laser pulses (YL593T3-030FC, Shanghai Laser & Optics Century Co.) at 0.45 mW/fiber for 30 seconds every 20 minutes for 8 hours using custom-made MATLAB software (Mathworks). The protocol is illustrated in Fig. 1.

2.5. Histology and immunohistochemistry

Mice were perfused transcardially using 4 % paraformaldehyde in phosphate buffered saline (PBS). The dissected brains were then incubated in the same solution for 12 hours, and subsequently sectioned coronally at 50 μ m thickness using a vibratome. For c-Fos immunohistochemistry, two or three sections between + 0.5 and + 1.0 mm AP per animal were selected and incubated in a buffer composed of 0.1 M Tris-HCl, 0.15 M NaCl, 0.5 % Triton-X, 5 % blocking reagent (Roche) with primary antibody (rabbit, polyclonal. 1:500, catalog #2250S, Cell Signaling) overnight at 4 °C. The sections were rinsed with PBS 3 times for 10 minutes, incubated with Alexa Fluor Plus 488 conjugated secondary antibody against rabbit IgG (goat, 1:200, catalog #A-11008, Thermo Fisher) and Hoechst 33258 for 2 hours and rinsed again with PBS as above. Tile-scan images were acquired using confocal microscopy (FV1200 and IX83, Olympus) using 10 \times objective lens (at 15 \times digital zoom). Image J was used to calculate the total nuclei and c-Fos positive cells in a 0.4 \times 0.4 mm² region of the ACC. Layer 2/3 was defined as depths ranging 100–350 μ m from the cortical surface and layer 5 as depths greater than 350 μ m (Muñoz et al., 2017).

2.6. Statistical analysis

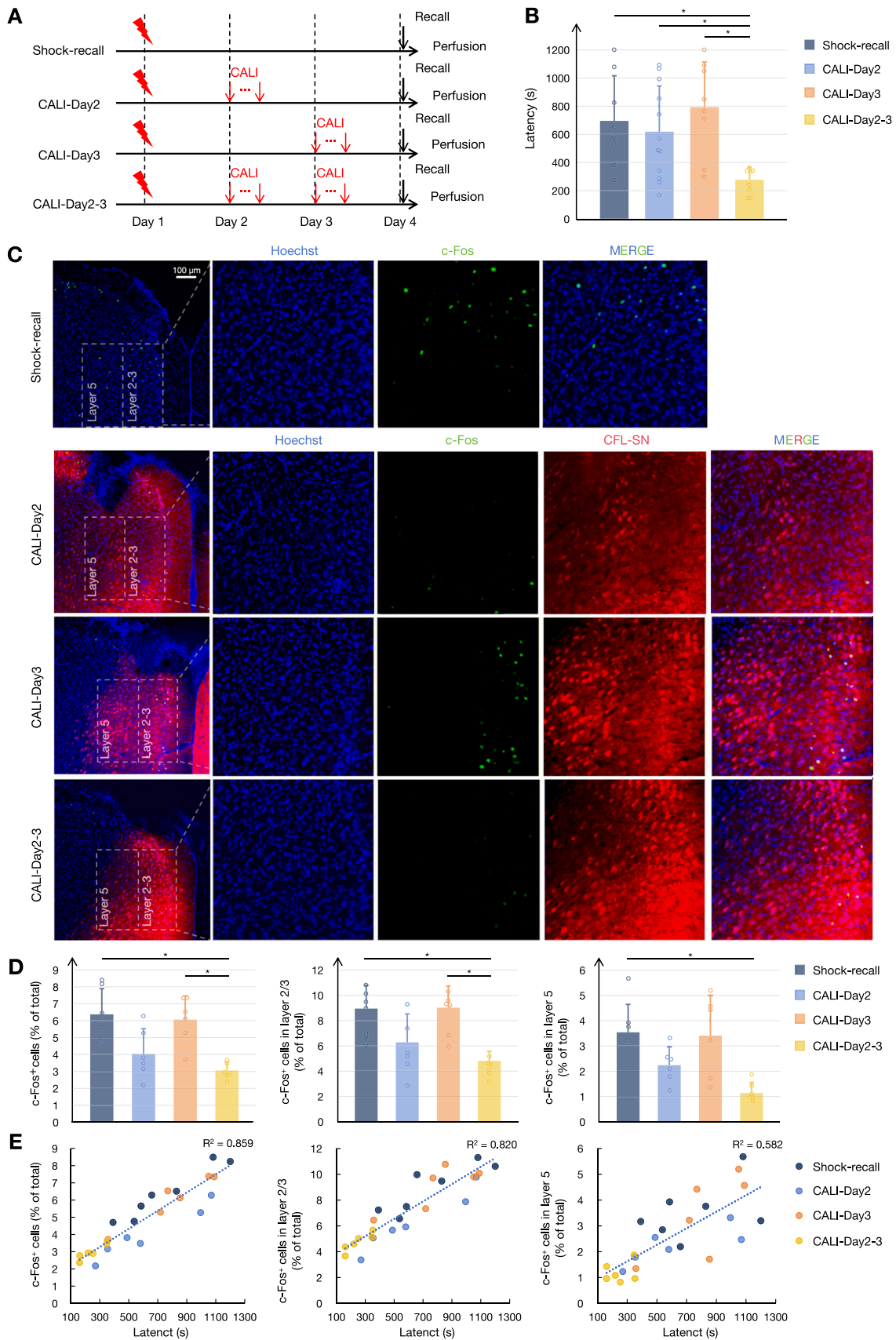
Statistical analyses were performed using IBM SPSS software version 25.0. Data are presented as mean \pm standard error. The Wilcoxon rank-sum test was used for comparison among different groups. Statistical significance was set at two-side $p < 0.05$. The Bonferroni correction was applied when comparing more than two groups. Simple linear regression analysis was performed to explore the correlation between crossover latency during memory recall and the proportion of c-Fos⁺ cells. In figures, statistically significant difference is indicated by an asterisk (*), and detailed statistical information, including sample sizes, p values and adjusted α threshold levels, are provided in the figure legends.

3. Results

3.1. CALI in ACC impairs memory

We expressed CFL-SN in dorsal ACC of mice by locally injecting AAV vectors, primarily targeting the Cg1 area, and implanted a dual-fiber cannula above the injection site. The IA learning was conducted two weeks post-surgery. On day 1, mice were exposed to the context paired with foot shocks. On day 2, during the diurnal cycle when mice typically sleep, they were illuminated with 594 nm laser to induce CALI for 30 sec every 20 min over an 8-hour period. In the previous study, we implanted electrodes together with optical cannula and performed online Fourier analysis of electroencephalogram and electromyogram to detect sleep (Goto et al., 2021). This showed that CALI during the sleep period impairs memory, but not during the awake period. Therefore, in the current study, illumination was repeated every 20 min during the diurnal period. On day 3, memory was assessed by measuring the crossover latency to the dark side of the chamber (Fig. 1). The illumination effectively erased memory in both CaMKII-Cre mice injected with AAV₂-EF1 α -DOI-CFL-SN (Fig. S1; shock-CALI-recall group, 150.7 \pm 102.1 s; shock-recall group, 770.0 \pm 439.0 s; $p = 0.014$). Essentially the same result was obtained with WT mice injected with AAV₂-CaMKII-CFL-SN (Fig. 2A-C; shock-CALI-recall group, 251.5 \pm 84.0 s; shock-recall group, 612.3 \pm 404.9 s; $p = 0.009$), consistent with our previous findings (Goto et al., 2021) that CALI in the ACC impairs fear memory. Because these two mouse lines exhibited consistent results, for the rest of study, we used WT mice with AAV₂-CaMKII-CFL-SN.

In addition to the behavioral assessment, we monitored the formation of engram cells in the ACC by staining tissues fixed 90 min after memory recall with a c-Fos antibody (Zhang et al., 2002). Consistent with the behavior result (Grella et al., 2020; Jhang et al., 2018), the proportion of c-Fos⁺ cells significantly increased in the shock-recall group (6.5 \pm 1.9 %) compared with naïve groups (1.5 \pm 0.3 %; $p = 0.002$). This increase was evident in both layer 2/3 (naïve group: 1.8 \pm 0.5 %; shock-recall group: 7.8 \pm 2.2 %; $p = 0.002$) and layer 5 (naïve group: 1.2 \pm 0.2 %; shock-recall group: 4.5 \pm 0.5 %; $p = 0.002$). Meanwhile, a higher proportion of c-Fos⁺ cells was observed in layer 2/3 compared to layer 5 (Fig. 2D and E). The elevated c-Fos expression was attributed to the neuronal activity associated with memory recall, as the shock-only group (without recall) exhibited comparable to those of naïve animals (2.1 \pm 0.1 % in all layers, 2.7 \pm 0.3 % in layer 2/3 and 1.4 \pm 0.4 % in layer 5; no significant differences from the naïve group). In contrast, the proportion of c-Fos⁺ cells was largely suppressed in the shock-CALI-recall group (2.6 \pm 0.4 % in all layers; $p_{\text{v.s. Naïve}} = 0.002$; $p_{\text{v.s. shock-recall}} = 0.002$; 3.5 \pm 0.4 % in layer 2/3 and 1.7 \pm 0.6 % in layer 5) (Fig. 2D and E). These results align closely with the behavior changes observed, as a statistically significant correlation was observed between the proportion of c-Fos⁺ cells and crossover latency to the dark chamber, suggesting a causal relationship (Fig. 2F).



(caption on next page)

Fig. 3. Memory can be reinstated by allowing one extra day after CALI on day 2.(A). Experimental protocols for the four groups: shock-recall (mice without surgery, subjected to shock and memory recall), CALI-Day2 (mice expressing CFL-SN, shocked, illuminated on day 2, followed by recall on day 4), CALI-Day3 (mice expressing CFL-SN, shocked, illuminated on day 3, followed by recall on day 4), and CALI-Day2-3 (mice expressing CFL-SN, shocked, illuminated on both day 2 and 3, followed by recall on day 4). (B) Memory recall on day 4 was assessed across the groups using the Wilcoxon rank-sum test, indicating that memory could only be erased in CALI-Day2-3 group ($n_{\text{shock-recall}} = 8; n_{\text{CALI-Day2}} = 12; n_{\text{CALI-Day3}} = 8; n_{\text{CALI-Day2-3}} = 8; p_{\text{shock-recall v.s. CALI-Day2}} = 0.521; p_{\text{shock-recall v.s. CALI-Day3}} = 0.505; p_{\text{shock-recall v.s. CALI-Day2-3}} = 0.002; p_{\text{CALI-Day2 v.s. CALI-Day3}} = 0.270; p_{\text{CALI-Day2 v.s. CALI-Day2-3}} = 0.010; p_{\text{CALI-Day3 v.s. CALI-Day2-3}} = 0.003$). The α threshold was set at 0.0083 (0.05/6). (C) c-Fos immunoreactivity of ACC cells across the groups. (D) Proportions of c-Fos⁺ cells relative to total cells (left) in each group were compared using the Wilcoxon rank-sum test ($n_{\text{shock-recall}} = 7$ mice; $n_{\text{CALI-Day2}} = 6$ mice; $n_{\text{CALI-Day3}} = 6$ mice; $n_{\text{CALI-Day2-3}} = 6$ mice; $p_{\text{shock-recall v.s. CALI-Day2}} = 0.022; p_{\text{shock-recall v.s. CALI-Day3}} = 1.000; p_{\text{shock-recall v.s. CALI-Day2-3}} = 0.001; p_{\text{CALI-Day2 v.s. CALI-Day3}} = 0.041; p_{\text{CALI-Day2 v.s. CALI-Day2-3}} = 0.180; p_{\text{CALI-Day3 v.s. CALI-Day2-3}} = 0.002$) in all layers as well as those separating by layer 2/3 (middle; $p_{\text{shock-recall v.s. CALI-Day2}} = 0.051; p_{\text{shock-recall v.s. CALI-Day3}} = 1.000; p_{\text{shock-recall v.s. CALI-Day2-3}} = 0.001; p_{\text{CALI-Day2 v.s. CALI-Day3}} = 0.041; p_{\text{CALI-Day2 v.s. CALI-Day2-3}} = 0.180; p_{\text{CALI-Day3 v.s. CALI-Day2-3}} = 0.002$) and layer 5 cells (right; $p_{\text{shock-recall v.s. CALI-Day2}} = 0.035; p_{\text{shock-recall v.s. CALI-Day3}} = 0.945; p_{\text{shock-recall v.s. CALI-Day2-3}} = 0.001; p_{\text{CALI-Day2 v.s. CALI-Day3}} = 0.310; p_{\text{CALI-Day2 v.s. CALI-Day2-3}} = 0.015; p_{\text{CALI-Day3 v.s. CALI-Day2-3}} = 0.015$). The α threshold was set at 0.0083 (0.05/6). A higher proportion of c-Fos⁺ cells was observed in layer 2/3 compared to layer 5 ($p_{\text{shock-recall}} = 0.001; p_{\text{CALI-Day2}} = 0.002; p_{\text{CALI-Day3}} = 0.002; p_{\text{CALI-Day2-3}} = 0.002$), and α threshold was set at 0.05. (E) The crossover latency of recall on day 4 showed a significant correlation with the proportion of c-Fos⁺ cells in the ACC (left; $p < 0.001; R^2 = 0.859$), layer 2/3 (middle; $p < 0.001; R^2 = 0.820$), and layer 5 (right; $p < 0.001; R^2 = 0.582$).

3.2. Memory is reinstated by allowing one extra day after CALI on day 2

When LTP in the ACC is blocked on day 2, memory recall is impaired (Fig. 2). However, the memory may still reside in the hippocampus or elsewhere in the brain and could potentially still be recalled if LTP occurs in ACC after day 2. To investigate this possibility, following CALI on day 2, mice were left in their home cages on day 3 without CALI, and the memory was assessed on day 4 (Fig. 3A). Despite erasure of LTP on day 2, memory could be recalled on day 4 to a level comparable to the shock-recall group (CALI-Day2 group, 619.0 ± 325.2 s; shock-recall group, 696.0 ± 320.2 s; $p = 0.521$; Fig. 3B). However, when CALI was administered consecutively on both days 2 and 3, memory could not be recalled on day 4 (CALI-Day2-3 group, 277.3 ± 89.1 s; $p_{\text{v.s. shock-recall}} = 0.002$; Fig. 3B). Taken together with the observation that when LTP was erased on day 2 and recall was tested on day 3, the animals could not recall the memory (Fig. 2), these findings indicate that, in animals that received CALI on day 2, though the memory remains in the brain on day 3, it is not in a form readily retrievable. LTP in ACC in at least one additional day is required to make it retrievable. Additionally, another group of mice were left in home cages on day 2 followed by CALI on day 3, their memory could also be recalled on day 4 (CALI-Day3 group, 793.8 ± 327.6 s; $p_{\text{v.s. shock-recall}} = 0.505; p_{\text{v.s. CALI-Day2}} = 0.270; p_{\text{v.s. CALI-Day2-3}} = 0.003$; Fig. 3B). This reveals that once LTP takes place in the ACC without the manipulation of CALI, the associated memory can be recalled starting from the following day.

The proportion of c-Fos⁺ cells was significantly reduced in CALI-Day2-3 groups compared to the shock-recall or CALI-Day3 animals (shock-recall group, 6.3 ± 1.5 %; CALI-Day3, 6.1 ± 1.4 %; CALI-Day2-3, 3.1 ± 0.5 %; $p_{\text{v.s. shock-recall}} = 0.001; p_{\text{v.s. CALI-Day3}} = 0.002$; Fig. 3C and D). Consistently, when the CALI-Day2 group was included in the comparisons, the c-Fos⁺ cell proportions showed no significant differences (CALI-Day2: 4.0 ± 1.5 %; $p_{\text{v.s. shock-recall}} = 0.022; p_{\text{v.s. CALI-Day3}} = 0.041; p_{\text{v.s. CALI-Day2-3}} = 0.180$; Fig. 3D). When plotting the relationship between crossover latency, the fraction of c-Fos⁺ cells revealed a strong correlation (Fig. 3E).

3.3. Memory can be still reinstated after a week of CALI by allowing one day for consolidation

The above findings prompted us to investigate how long memories are retained in the hippocampus or elsewhere in brain. To this end, we administered 8-hour CALI for seven consecutive days following the learning session from day 2 to day 8 and performed the recall session on day 9 (Fig. 4A). This significantly shortened the crossover latency in the illuminated mice (214.0 ± 133.8 s) compared to the shock-recall group indicating that the memory was erased (743.4 ± 338.0 s; $p = 0.003$; Fig. 4B). However, when the animals were kept in their home cages for one additional day without CALI and exposed to the context on day 10, they could recall the memory (977.8 ± 212.3 s; $p = 0.002$; Fig. 4B). Furthermore, a strong correlation was seen between crossover latency

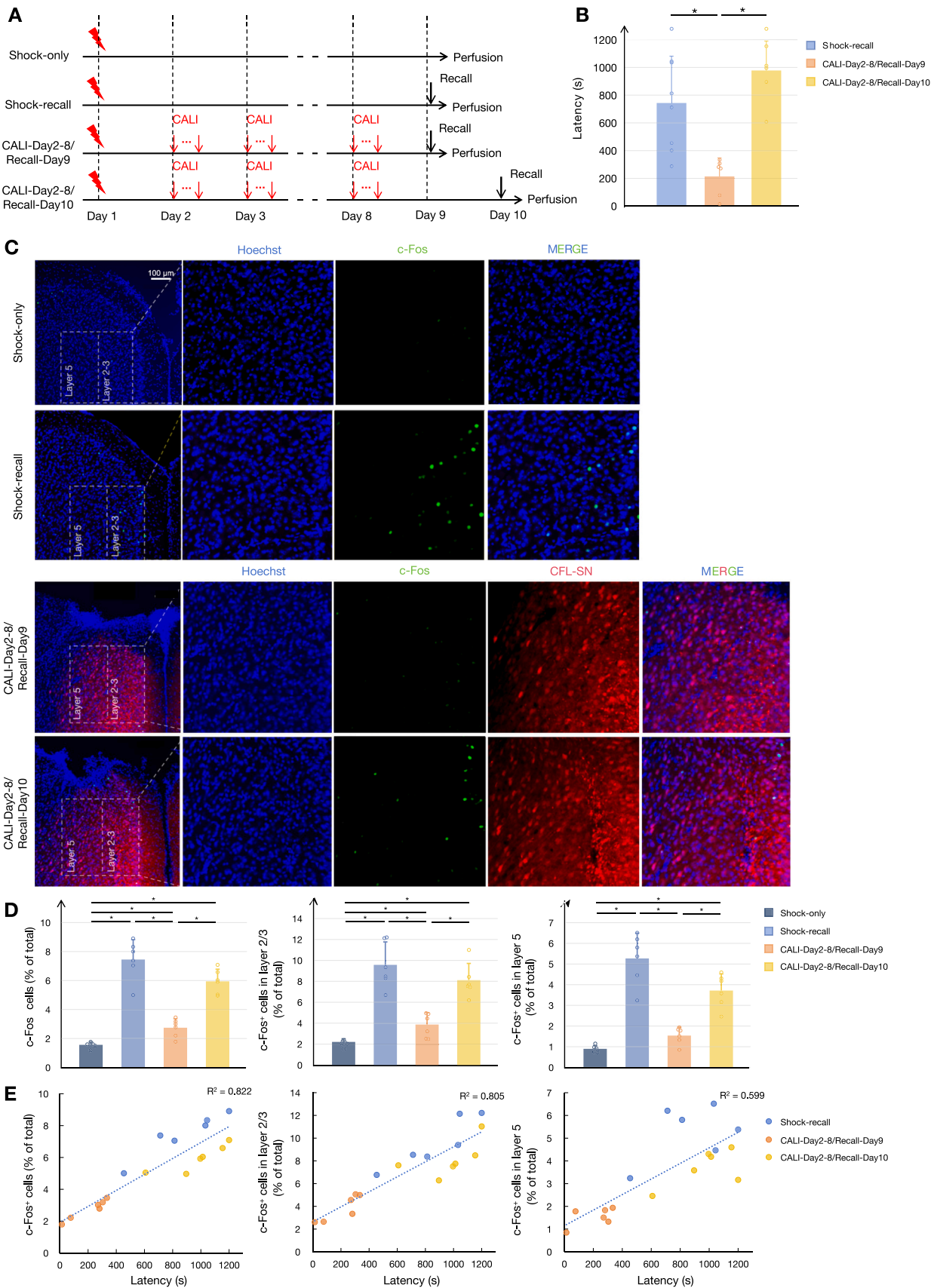
and the fraction of c-Fos positive cells (Fig. 4C to E). These results indicate that the memory was retained in the brain up to 9 days post-learning in a form that can evoke LTP in the ACC.

4. Discussion

By employing a unique optogenetic tool, CFL-SN, to selectively erase LTP in excitatory neurons, we identified the time window when LTP occurs in the ACC. We previously demonstrated that LTP in the ACC takes place during sleep on the second day after learning (Goto et al., 2021). Extending this analysis, we found that memory was impaired when CALI in the ACC was applied over a 2–8 day period. However, allowing one extra day without CALI to allow the memory to consolidate in ACC, resulted in reinstatement of the memory. This implies that even if a memory is not immediately consolidated in the ACC after prolonged CALI, it remains stored in the brain in a form that is insufficient for retrieval to elicit appropriate behavior responses.

At this point, it is unclear where the memory is retained before it is transferred to the ACC. One potential candidate is the hippocampus itself, where it has been demonstrated using calcium-imaging, that the activity of place cells towards behaviorally relevant spaces or cues tends to be stable over days, while the representation for neural location gradually drifts (Sato et al., 2020; Ziv et al., 2013). This demonstrates that the hippocampus has the ability to retain a similar representation over days, aligning with the findings from a recent study (Shin et al., 2024). Memory retention may also exist in other brain regions. The direct connections from the hippocampus to the ACC are relatively limited, primarily arising from the ventral hippocampus (Hoover and Vertes, 2007; Meyer et al., 2019) and the projections from the dorsal hippocampus are mediated through the retrosplenial cortex, which is bidirectionally connected with both the hippocampus and the ACC (Lee et al., 2023). Therefore, it could be argued that the memory is retained in the retrosplenial cortex, which can be addressed in future studies by targeting LTP in retrosplenial cortex using CFL-SN, in similar manner.

Our results also indicate that even though memories are retained, they are insufficient to induce recall unless the memory is transferred to the ACC. Why this is the case remains unclear. One possible explanation is that, since ACC modulation can directly influence the ability to retrieve fear memories (Liu et al., 2009), task acquisition may trigger semi-persistent changes in ACC firing patterns acting as a short-term store of an aversive event. Under normal circumstances the induction of LTP during sleep would facilitate the long-term transfer of this memory to ACC, altering the synaptic weights of the activity tagged neurons, and potentially resetting their firing rates back to basal levels. Since CALI precludes the expression of LTP in ACC, it could be argued that the any resultant task dependent changes in ACC firing may thus persist and interfere with memory recall. To further investigate the role of offline LTP in ACC engram cells, future studies could employ chemogenetic activation of these neurons to determine whether offline engrams in the ACC are critical for memory recall. Notably, our data



(caption on next page)

Fig. 4. Memory can be still reinstated after a week of CALI by allowing one extra day. Experimental protocols for the three groups: shock-only (mice without surgery, subjected to shock on day 1), shock-recall (mice without surgery, subjected to shock on day 1, and memory recall on day 9), CALI-Day2–8/Recall-Day9 (mice expressing CFL-SN, shocked, illuminated only on day 2–8, followed by recall in day 9) and CALI-Day2–8/Recall-Day10 (mice expressing CFL-SN, shocked, illuminated on day 2–8, followed by recall on day 10). **(B)** Crossover latency in memory recall was compared among the three groups using the Wilcoxon rank-sum test, indicating that memory could only be erased in CALI-Day2–8/Recall-Day9 group ($n_{\text{shock-recall}} = 8$; $n_{\text{CALI-Day2-8/Recall-Day9}} = 6$; $n_{\text{CALI-Day2-8/Recall-Day10}} = 6$; $p_{\text{shock-recall v.s. CALI-Day2-8/Recall-Day9}} = 0.003$; $p_{\text{shock-recall v.s. CALI-Day2-8/Recall-Day10}} = 0.282$; $p_{\text{CALI-Day2-8/Recall-Day9 v.s. CALI-Day2-8/Recall-Day10}} = 0.002$). The α threshold was set at 0.0167 (0.05/3). **(C)** c-Fos immunoreactivity of cells across the three groups. **(D)** Proportions of c-Fos⁺ cells relative to total cells (left) in each group were compared using the Wilcoxon rank-sum test ($n_{\text{shock-only}} = 6$ mice; $n_{\text{shock-recall}} = 6$ mice; $n_{\text{CALI-Day2-8/Recall-Day9}} = 6$ mice; $n_{\text{CALI-Day2-8/Recall-Day10}} = 6$ mice; $p_{\text{shock-only v.s. shock-recall}} = 0.002$; $p_{\text{shock-only v.s. CALI-Day2-8/Recall-Day9}} = 0.002$; $p_{\text{shock-only v.s. CALI-Day2-8/Recall-Day10}} = 0.002$; $p_{\text{shock-recall v.s. CALI-Day2-8/Recall-Day9}} = 0.002$; $p_{\text{shock-recall v.s. CALI-Day2-8/Recall-Day10}} = 0.065$; $p_{\text{CALI-Day2-8/Recall-Day9 v.s. CALI-Day2-8/Recall-Day10}} = 0.002$), as well as those separating by layer 2/3 (middle; $p_{\text{shock-only v.s. shock-recall}} = 0.002$; $p_{\text{shock-only v.s. CALI-Day2-8/Recall-Day9}} = 0.002$; $p_{\text{shock-only v.s. CALI-Day2-8/Recall-Day10}} = 0.002$; $p_{\text{shock-recall v.s. CALI-Day2-8/Recall-Day9}} = 0.002$; $p_{\text{shock-recall v.s. CALI-Day2-8/Recall-Day10}} = 0.180$; $p_{\text{CALI-Day2-8/Recall-Day9 v.s. CALI-Day2-8/Recall-Day10}} = 0.002$) or layer 5 (right; $p_{\text{shock-only v.s. shock-recall}} = 0.002$; $p_{\text{shock-only v.s. CALI-Day2-8/Recall-Day9}} = 0.026$; $p_{\text{shock-only v.s. CALI-Day2-8/Recall-Day10}} = 0.002$; $p_{\text{shock-recall v.s. CALI-Day2-8/Recall-Day9}} = 0.002$; $p_{\text{shock-recall v.s. CALI-Day2-8/Recall-Day10}} = 0.065$; $p_{\text{CALI-Day2-8/Recall-Day9 v.s. CALI-Day2-8/Recall-Day10}} = 0.002$). The α threshold was set at 0.0083 (0.05/6). A higher proportion of c-Fos⁺ cells was observed in layer 2/3 compared to layer 5 ($p_{\text{shock-only}} = 0.002$; $p_{\text{shock-recall}} = 0.002$; $p_{\text{CALI-Day2-8/Recall-Day9}} = 0.002$; $p_{\text{CALI-Day2-8/Recall-Day10}} = 0.002$), and α threshold was set at 0.05. **(E)** The crossover latency of recall on day 9/10 was significantly correlated with the proportion of c-Fos⁺ cells in the ACC (left; $p < 0.001$; $R^2 = 0.822$), layer 2/3 (middle; $p < 0.001$; $R^2 = 0.805$), and layer 5 (right; $p < 0.001$; $R^2 = 0.599$).

demonstrate that memories can be retained in the brain for long periods (up to 8 days) despite the absence of LTP in the ACC. Overall these findings provide insight into the role of ACC during the memory consolidation, significantly enhancing our understanding of behavioral responses in adverse conditions.

CRedit authorship contribution statement

Junyu Liu: Writing – review & editing, Writing – original draft, Visualization, Validation, Software, Methodology, Investigation, Funding acquisition, Formal analysis, Data curation, Conceptualization. **Akihiro Goto:** Writing – review & editing, Writing – original draft, Visualization, Supervision, Methodology, Investigation, Funding acquisition, Conceptualization. **Yasunori Hayashi:** Writing – review & editing, Writing – original draft, Visualization, Validation, Supervision, Project administration, Methodology, Investigation, Funding acquisition, Conceptualization.

Declaration of Competing Interest

None.

Acknowledgement

We thank Nozomi Asaoka for her assistance in constructing the AAV vector and Steven J. Middleton for comments on the manuscript. This work was supported by the Grant-in-Aid for JSPS Fellows JP24KJ1400 (J.L.); Grants-in-Aid for Scientific Research JP22H02720, JP22H05496, and JP24K22001 from MEXT, Japan, JST PRESTO grant number JPMJPR22S5, The Takeda Science Foundation, Research Foundation for Opto-Science and Technology, Narishige Foundation, Kishimoto Foundation, and Sumitomo Foundation (A.G.); Grants-in-Aid for Scientific Research P18H05434, JP20K21462, JP22H04981 and JP22K21353, from the MEXT, Japan, The Uehara Memorial Foundation, The Naito Foundation, Research Foundation for Opto-Science and Technology, Novartis Foundation, and The Takeda Science Foundation, HFSP Research Grant RGP0022/2013, and JST CREST JPMJCR20E4 (Y.H.).

Appendix A. Supporting information

Supplementary data associated with this article can be found in the online version at [doi:10.1016/j.neures.2024.12.009](https://doi.org/10.1016/j.neures.2024.12.009).

Data availability

All data are available upon reasonable request.

References

- Bero, A.W., Meng, J., Cho, S., Shen, A.H., Canter, R.G., Ericsson, M., Tsai, L.H., 2014. Early remodeling of the neocortex upon episodic memory encoding. *Proc. Natl. Acad. Sci. USA* 111 (32), 11852–11857. <https://doi.org/10.1073/pnas.1408378111>.
- Bontempi, B., Laurent-Demir, C., Destrade, C., Jaffard, R., 1999. Time-dependent reorganization of brain circuitry underlying long-term memory storage. *Nature* 400 (6745), 671–675. <https://doi.org/10.1038/23270>.
- Bosch, M., Castro, J., Saneyoshi, T., Matsuno, H., Sur, M., Hayashi, Y., 2014. Structural and molecular remodeling of dendritic spine substructures during long-term potentiation. *Neuron* 82 (2), 444–459. <https://doi.org/10.1016/j.neuron.2014.03.021>.
- Frankland, P.W., Bontempi, B., Talton, L.E., Kaczmarek, L., Silva, A.J., 2004. The involvement of the anterior cingulate cortex in remote contextual fear memory. *Science* 304 (5672), 881–883. <https://doi.org/10.1126/science.1094804>.
- Frankland, P.W., Bontempi, B., 2005. The organization of recent and remote memories. *Nat. Rev. Neurosci.* 6 (2), 119–130. <https://doi.org/10.1038/nrn1607>.
- Frankland, P.W., O'Brien, C., Ohno, M., Kirkwood, A., Silva, A.J., 2001. Alpha-CaMKII-dependent plasticity in the cortex is required for permanent memory. *Nature* 411 (6835), 309–313. <https://doi.org/10.1038/35077089>.
- Goto, A., 2022. Synaptic plasticity during systems memory consolidation. *Neurosci. Res* 183, 1–6. <https://doi.org/10.1016/j.neures.2022.05.008>.
- Goto, A., Bota, A., Miya, K., Wang, J., Tsukamoto, S., Jiang, X., Hirai, D., Murayama, M., Matsuda, T., McHugh, T.J., Nagai, T., Hayashi, Y., 2021. Stepwise synaptic plasticity events drive the early phase of memory consolidation. *Science* 374 (6569), 857–863. <https://doi.org/10.1126/science.abj9195>.
- Grella, S.L., Fortin, A.H., McKissick, O., Leblanc, H., Ramirez, S., 2020. Odor modulates the temporal dynamics of fear memory consolidation. *Learn Mem.* 27 (4), 150–163. <https://doi.org/10.1101/lm.050690.119>.
- Grieger, J.C., Choi, V.W., Samulski, R.J., 2006. Production and characterization of adeno-associated viral vectors. *Nat. Protoc.* 1 (3), 1412–1428. <https://doi.org/10.1038/nprot.2006.207>.
- Hoover, W.B., Vertes, R.P., 2007. Anatomical analysis of afferent projections to the medial prefrontal cortex in the rat. *Brain Struct. Funct.* 212 (2), 149–179. <https://doi.org/10.1007/s00429-007-0150-4>.
- Jhang, J., Lee, H., Kang, M.S., Lee, H.S., Park, H., Han, J.H., 2018. Anterior cingulate cortex and its input to the basolateral amygdala control innate fear response. *Nat. Commun.* 9 (1), 2744. <https://doi.org/10.1038/s41467-018-05090-y>.
- Kim, K., Lakhanpal, G., Lu, H.E., Khan, M., Suzuki, A., Hayashi, M.K., Narayanan, R., Luyben, T.T., Matsuda, T., Nagai, T., Blanpied, T.A., Hayashi, Y., Okamoto, K., 2015. A Temporary Gating of Actin Remodeling during Synaptic Plasticity Consists of the Interplay between the Kinase and Structural Functions of CaMKII. *Neuron* 87 (4), 813–826. <https://doi.org/10.1016/j.neuron.2015.07.023>.
- Kitamura, T., Ogawa, S.K., Roy, D.S., Okuyama, T., Morrissey, M.D., Smith, L.M., Redondo, R.L., Tonegawa, S., 2017. Engrams and circuits crucial for systems consolidation of a memory. *Science* 356 (6333), 73–78. <https://doi.org/10.1126/science.aam6808>.
- Lee, J.H., Kim, W.B., Park, E.H., Cho, J.H., 2023. Neocortical synaptic engrams for remote contextual memories. *Nat. Neurosci.* 26 (2), 259–273. <https://doi.org/10.1038/s41593-022-01223-1>.
- Liu, F., Zheng, X.L., Li, B.M., 2009. The anterior cingulate cortex is involved in retrieval of long-term/long-lasting but not short-term memory for step-through inhibitory avoidance in rats. *Neurosci. Lett.* 460 (2), 175–179. <https://doi.org/10.1016/j.neulet.2009.05.032>.
- Meyer, H.C., Odriozola, P., Cohodes, E.M., Mandell, J.D., Li, A., Yang, R., Hall, B.S., Haberman, J.T., Zacharek, S.J., Liston, C., Lee, F.S., Gee, D.G., 2019. Ventral hippocampus interacts with prelimbic cortex during inhibition of threat response via learned safety in both mice and humans. *Proc. Natl. Acad. Sci. USA* 116 (52), 26970–26979. <https://doi.org/10.1073/pnas.1910481116>.
- Muñoz, W., Tremblay, R., Levenstein, D., Rudy, B., 2017. Layer-specific modulation of neocortical dendritic inhibition during active wakefulness. *Science* 355 (6328), 954–959. <https://doi.org/10.1126/science.aag2599>.

- Rolls, E.T., 2023. Emotion, motivation, decision-making, the orbitofrontal cortex, anterior cingulate cortex, and the amygdala. *Brain Struct. Funct.* 228 (5), 1201–1257. <https://doi.org/10.1007/s00429-023-02644-9>.
- Sakaguchi, M., Hayashi, Y., 2012. Catching the engram: strategies to examine the memory trace. *Mol. Brain* 5, 32. <https://doi.org/10.1186/1756-6606-5-32>.
- Sato, M., Mizuta, K., Islam, T., Kawano, M., Sekine, Y., Takekawa, T., Gomez-Dominguez, D., Schmidt, A., Wolf, F., Kim, K., Yamakawa, H., Ohkura, M., Lee, M.G., Fukai, T., Nakai, J., Hayashi, Y., 2020. Distinct Mechanisms of Over-Representation of Landmarks and Rewards in the Hippocampus. *Cell Rep.* 32 (1), 107864. <https://doi.org/10.1016/j.celrep.2020.107864>.
- Shin, M.E., Parra-Bueno, P., Yasuda, R., 2024. Formation of long-term memory without short-term memory revealed by CaMKII inhibition (Published online.). *Nat. Neurosci.* <https://doi.org/10.1038/s41593-024-01831-z>.
- Smith, M.L., Asada, N., Malenka, R.C., 2021. Anterior cingulate inputs to nucleus accumbens control the social transfer of pain and analgesia. *Science* 371 (6525), 153–159. <https://doi.org/10.1126/science.abe3040>.
- Takemoto, K., Matsuda, T., Sakai, N., Fu, D., Noda, M., Uchiyama, S., Kotera, I., Arai, Y., Horiuchi, M., Fukui, K., Ayabe, T., Inagaki, F., Suzuki, H., Nagai, T., 2013. SuperNova, a monomeric photosensitizing fluorescent protein for chromophore-assisted light inactivation. *Sci. Rep.* 3, 2629. <https://doi.org/10.1038/srep02629>.
- Toader, A.C., Regalado, J.M., Li, Y.R., Terceros, A., Yadav, N., Kumar, S., Satow, S., Hollunder, F., Bonito-Oliva, A., Rajasethupathy, P., 2023. Anteromedial thalamus gates the selection and stabilization of long-term memories. *e1317 Cell* 186 (7), 1369–1381. <https://doi.org/10.1016/j.cell.2023.02.024>.
- Tonegawa, S., Morrissey, M.D., Kitamura, T., 2018. The role of engram cells in the systems consolidation of memory. *Nat. Rev. Neurosci.* 19 (8), 485–498. <https://doi.org/10.1038/s41583-018-0031-2>.
- Tsien, J.Z., Huerta, P.T., Tonegawa, S., 1996. The essential role of hippocampal CA1 NMDA receptor-dependent synaptic plasticity in spatial memory. *Cell* 87 (7), 1327–1338. [https://doi.org/10.1016/s0092-8674\(00\)81827-9](https://doi.org/10.1016/s0092-8674(00)81827-9).
- Wu, K., Wang, D., Wang, Y., Tang, P., Li, X., Pan, Y., Tao, H.W., Zhang, L.I., Liang, F., 2023. Distinct circuits in anterior cingulate cortex encode safety assessment and mediate flexibility of fear reactions. *e3656 Neuron* 111 (22), 3650–3667. <https://doi.org/10.1016/j.neuron.2023.08.008>.
- Zhang, J., Zhang, D., McQuade, J.S., Behbehani, M., Tsien, J.Z., Xu, M., 2002. c-fos regulates neuronal excitability and survival. *Nat. Genet* 30 (4), 416–420. <https://doi.org/10.1038/ng859>.
- Ziv, Y., Burns, L.D., Cocker, E.D., Hamel, E.O., Ghosh, K.K., Kitch, L.J., El Gamal, A., Schnitzer, M.J., 2013. Long-term dynamics of CA1 hippocampal place codes. *Nat. Neurosci.* 16 (3), 264–266. <https://doi.org/10.1038/nn.3329>.